front where the lateral displacement is extremely small.

The source of the image was a grid of clear lines on relatively opaque 8 × 10 in. photographic film mounted vertically between glass plates and illuminated by an explosive argon flash lamp. The displacement of the image was observed with a Beckman–Whitley Model 189 Framing Camera. It was most convenient to mount the source grid parallel to the mirror plate as shown in Fig. 1. In this arrangement the length of the optical lever arm was identical for all points on the initial position of the plate and was given by the perpendicular distance from the plate to the grid. The deflection angle θ of the plate surface is then related to the vertical distance d by which the image is displaced by $\tan 2\theta = d/L$, where L is the plate-to-grid perpendicular distance. However, if the plate has been displaced outward a distance x, the relation is

$$\tan 2\theta = d/(L - x). \tag{1}$$

The displacement x was obtained by numerical integration of the experimental $\tan \theta$ versus y data

$$x = \int_0^y \tan \theta \, dy, \tag{2}$$

where y is the distance along the undeflected plate surface. A grid of crossed lines was used to enable separation of the vertical displacement of the image from a small horizontal displacement arising from the nonperpendicular angle of view in the horizontal plane and from any slight horizontal curvature of the plate. The scale for image displacement measurements was based on the vertical size of the undistorted grid as measured on the first frames of the sequence. Separate reference distances were provided (as shown in Fig. 2) for measurement of position on the plate. The camera was focussed to give a sharp image of the grid. The small vertical aperture of the framing camera provided a sharp vertical location of points on the plate, the lateral blurring being of no consequence. Motion blur of the displaced image was minimized by shortening the exposure time by reducing the vertical aperture to the point where diffraction began to degrade the spatial resolution. The quality of the reflecting surface of the plate often deteriorated considerably upon deformation, especially in the region slightly behind the detonation front where the acceleration was beginning to decrease from its maximum value. Figure 2 illustrates a typical frame from a framing camera sequence. In practice, a large number of readings of image displacement d versus distance y

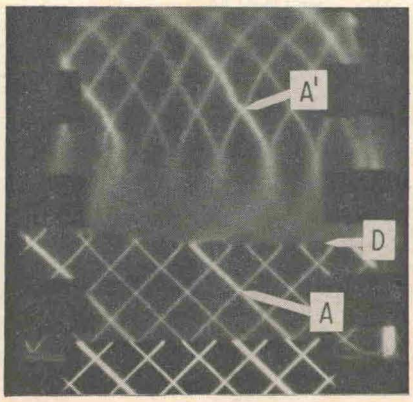

FIG. 2. Typical frame from framing camera sequence. The detonation front (D) is moving from top to bottom. The black rectangles on either side of the plate provide secondary distance references. Point A on undeflected image is equivalent to Point A′ on the deflected image. The displaced grid lines at the base of cell are lines reflected from a small mirror in front of the assembly, used to provide a fixed frame of reference for measurement if the detonation runs to the end.

behind the detonation front were taken from several frames (after a steady state configuration has been reached) in order to minimize the effects of local fluctuations in the explosive. A typical set of experimental d versus y values is shown in Fig. 3. Equations (1) and (2) were then used to obtain θ and x as functions of y.

The configuration of the explosive–metal interface and the pressure along it were determined by neglecting the thickness of the plate. This assumption, while intuitively reasonable, is difficult to justify in a quantitative way. It would be possible to treat the plate as either an incompressible or compressible fluid in steady flow and compute both the configuration of and the pressure along the explosive–metal interface. However, it is not clear how to take account of the elastic strength of the plate in a detailed

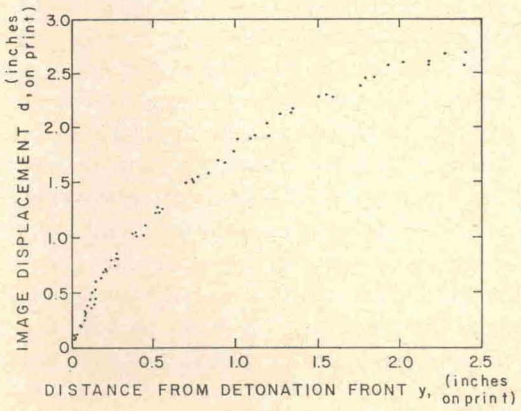

FIG. 3. Example of typical experimental data of image displacement versus distance behind the detonation front.

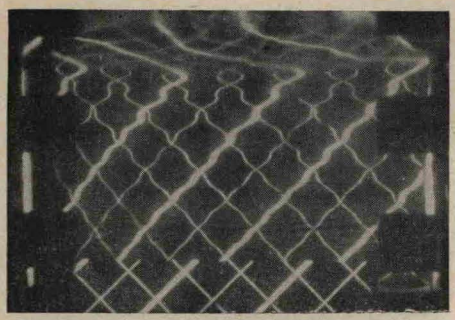

FIG. 4. Frame illustrating elastic bending wave pattern set up in stainless-steel plate when the detonation velocity is less than about 2.0 mm/μsec.

way. It was therefore chosen to use the zero thickness approximation rather than to make an elaborate partial correction.

The energy dissipated in plastic deformation may be estimated roughly by computing the energy required to bend the plate to maximum curvature and to straighten it. In typical experiments, this estimate is only 1 or 2 cal/g of explosive, which is less than 1% of the observed kinetic energy of the plates per gram of explosive. When the detonation velocity D exceeds the shear wave velocity of the plate metal, the only elastic disturbance in the plate that travels ahead of the detonation and is likely to be excited is a plate compressional wave. This symmetrical wave causes no net lateral displacement of the plate, but only an elastic thickening of the plate. The motion is too small to be observed by measurement of the surface angle. When the detonation velocity is less than the shear wave velocity, elastic bending waves can travel ahead of the detonation. We have observed these (Fig. 4) in stainless-steel plates only when the detonation velocity is less than 2.0 mm/μsec, compared with a shear wave velocity of about 3.1 mm/μsec. The only other effect of the elastic strength would be to contribute to a slight smearing of the measured pressure–distance profile in the region of the detonation front, where the rate of change of curvature is the highest. In this region the applied pressures are much larger than the elastic strength of the metal used for confinement. The assumption was thus made that the elastic properties of the walls had a negligible effect on the measured trajectory of the plates.

Since the plate does not elongate, the velocity vector of the plate is at an angle $\frac{1}{2}\theta$ with respect to the perpendicular to the initial plane of the plate and has a magnitude V_p given by

$$V_p = 2D \sin(\tfrac{1}{2}\theta), \tag{3}$$

where D is the detonation velocity. V_p was thus determined as a function of distance y behind the detonation front from the detonation velocity and the curve of θ as a function of y obtained as described earlier. The pressure on the plate as a function of distance behind the front was then obtained from

$$P \cos \tfrac{1}{2}\theta = m\, dV_p/dt = mD\, dV_p/dS, \tag{4}$$

where m is the mass of the plate per unit area and S is the distance along the deflected plate surface,

$$S = \int_0^y (1 + \tan^2 \theta)^{\frac{1}{2}}\, dy.$$

The quantity S is also derived from the tan θ versus y curve. In the present experiments cos $\frac{1}{2}\theta$ in Eq. (4) was essentially unity and was used as such in the analysis.

Analysis of Data

We obtain the dynamical behavior of the explosive in the detonation process from the pressure P, the lateral displacement x, and the detonation velocity D, by assuming that the flow of the explosive through the detonation can be analyzed as a pseudo one-dimensional channel flow (Fig. 5). In a coordinate system in which the detonation is stationary, the mass flow equation is

$$A\rho q = A_0\rho_0 D = A_0\rho_1 q_1, \tag{5}$$

where A is the cross-sectional area of the channel, ρ is the density, and q is the flow velocity. The subscript 0 refers to the explosive ahead of the detonation and the subscript 1 to the plane immediately behind the detonation front, where the cross-sectional area has not yet been increased by motion of the confining plates.

The equation of motion for one-dimensional channel flow is

$$-(1/\rho)\, dP/dS = q\, dq/dS. \tag{6}$$

For simplicity we set $P_0 = 0$ since $P_0 \ll P$. From

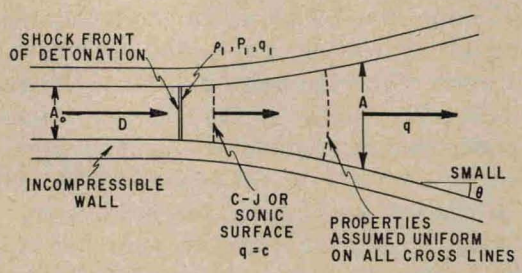

FIG. 5. Designation of parameters in pseudo one-dimensional channel flow treatment. Length of flow velocity vectors illustrates variation of flow rate through detonation front.